Obstacle Avoidance

Maria Isabel Ribeiro

3rd November 2005

1:1 Introduction

Given the a priori knowledge of the environment and the goal position, mobile robot navigation refers to the robot's ability to safely move towards the goal using its knowledge and the sensorial information of the surrounding environment.

Even though there are many different ways to approach navigation, most of them share a set of common components or blocks, among which path planning and obstacle avoidance (may) play a key role.

Given a map and a goal location, path planning involves finding a geometric path from the robot actual location to the goal. This is a global procedure whose execution performance is strongly dependent on a set of assumptions that are seldom observed in nowadays robots. In fact, in mobile robots operating in unstructured environments, or in service and companion robots, the a priori knowledge of the environment is usually absent or partial, the environment is not static, i.e., during the robot motion it can be faced with other robots, humans or pets, and execution is often associated with uncertainty. Therefore, for a collision free motion to the goal, the global path planning has to be associated with a local obstacle handling that involves obstacle detection and obstacle avoidance.

Obstacle avoidance refers to the methodologies of shaping the robot's path to overcome unexpected obstacles. The resulting motion depends on the robot actual location and on the sensor readings. There are a rich variety of algorithms for obstacle avoidance from basic re-planning to reactive changes in the control strategy. Proposed techniques differ on the use of sensorial data and on the motion control strategies to overcome obstacles.

The Bug's algorithms (section 2:1), [1], [2], follow the easiest common sense approach of moving directly towards the goal, unless an obstacle is found, in which case the obstacle is contoured until motion to goal is again possible. In these algorithms only the most recent values of sensorial data are used.

Path planning using artificial potential fields, [3], (section 2:2) is based on a simple and powerful principle that has an embedded obstacle avoidance capabil-

ity. The robot is consider as a particle that moves immersed in a potential field generated by the goal and by the obstacles present in the environment. The goal generates an attractive potential while each obstacle generates a repulsive potential. Obstacles are either a priori known, (and therefore the repulsive potential may be computed off-line) or on-line detected by the on-board sensors and therefore the repulsive potential is on-line evaluated. Besides the obstacle avoidance functionality, the potential field planning approach incorporates a motion control strategy that defines the velocity vector of the robot to drive it to the goal while avoiding obstacles.

The Vector Field Histogram, [4], (section 2:3) generates a polar histogram of the space occupancy in the close vicinity of the robot. This polar histogram, that is constructed around the robot's momentary location, is then checked to select the most suitable sector from among all polar histograms sectors with a low polar obstacle density and the steering of the robot is aligned with that direction.

Elastic bands [5] as a framework that combines the global path planning with a real-time sensor based robot control aiming at a collision free motion to the goal. An elastic band is a deformable collision-free path. According to [5], the initial shape of the elastic band is the free path generated by a planner. Whenever an obstacle is detected, the band is deformed according to an artificial force, aiming at keeping a smooth path and simultaneously maintaining the clearance from the obstacles. The elastic deforms as changes in the environment are detected by the sensors, enabling the robot to accommodate uncertainties and to avoid unexpected and moving obstacles.

A dynamic approach to behavior-based robotics proposed in [6], [7], models the behavior of a mobile robot as a non-linear dynamic system. The direction to the goal is set as a stable equilibrium point of this system while the obstacles impose an unstable equilibria point of this non-linear dynamics. The combination of both steers the robot to the goal while avoiding obstacles.

2:1 The Bug algorithms

The Bug algorithms, in its original version Bug 1, [1], or in the improved version Bug 2, [2], are simple ways to overcome unexpected obstacles in the robot motion from a start point s, to a goal point g. The goal of the algorithms is to generate a collision free path from the s to g with the underlying principle based on contouring the detected obstacles. The two versions of the algorithm differ on the conditions under which the border-following behavior is switched to the go-to-goal behavior.

Consider that the robot is a point operating in a plane, moving from s to g, and that it has a contact sensor or a zero range sensor to detect obstacles.

In the Bug 1 algorithm, as soon as an obstacle i is detected, the robot does a full contour around it, starting at the hit point H_i. This full contour aims at evaluating the point of minimum distance to the target, L_i. The robot then continues the contouring motion until reaching that point again, from where it leaves along a straight path to the target. L_i is named as the leave point. This technique is very inefficient but guarantees that the robot will reach any reachable goal. Figure 1 represents a situation with two obstacles where $H1$ and $H2$ are the hit points and $L1$ and $L2$ the leave points.

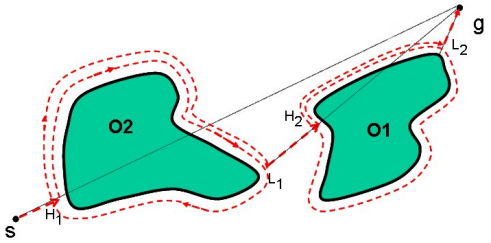

Figure 1: Obstacle avoidance with Bug 1 algorithm

In the Bug 2 algorithm the obstacle contour starts at the hit point H_i but ends whenever the robot crosses the line to the target. This defines the leave point L_i of the obstacle boundary-following behavior. From L_i the robot moves directly to the target. The procedure repeats if more obstacles are detected. Figure 2 represents the path generated by Bug 2 for two obstacles.

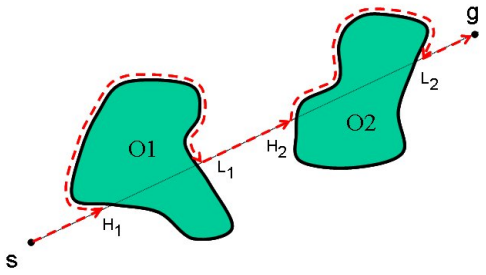

Figure 2: Obstacle avoidance with Bug 2 algorithm

In general, Bug 2 algorithm has a shorter travel time than Bug 1 algorithm and is more efficient specially in open spaces. However, there are situations where it may became non optimal. In particular, the robot may be trapped in maze structures.

The simplicity of these algorithms leads to a number of shortcomings. None of these algorithms take robot kinematics into account which is a severe limitation, specially in the case of non-holonomic robots. Moreover, and since only the most

recent sensorial data is taken into account, sensor-noise has a large impact in the robot performance.

For complete details of Bug 1 and Bug 2 see [1], [2], [8] and for extensions of Bug 2, in particular for a description of Tangent Bug that applies as a modification of the Bug 2 algorithm for non zero range sensors, see [9].

2:2 Potential Field Methods

Path planning using artificial potential fields is based on a simple and powerful principle, first proposed by O. Khatib in [3]. The robot is consider as a particle that moves immersed in a potential field generated by the goal and by the obstacles present in the environment. The goal generates an attractive potential while each obstacle generates a repulsive potential. A potential field can be viewed as an energy field and so its gradient, at each point, is a force. The robot immersed in the potential filed is subject to the action of a force that drives it to the goal (it is the action of the attractive force that results from the gradient of the attractive potential generated by the goal) while keeping it away from the obstacles (it is the action of a repulsive force that is the gradient of the repulsive potential generated by the obstacles).

The robot motion in potential field based methods can be interpreted as the motion of a particle in a gradient vector field generated by positive and negative electric particles. In this analogy, the robot is a positive charge, the goal is a negative charge and the obstacles are sets of positive charges. Gradients in this context can be interpreted as forces that attract the positively charged robot particle to a negative particle that acts as the goal. The obstacles act as positive charges that generate repulsive forces that force the particle robot away from the obstacles. The combination of the attractive force to the goal and the repulsive forces away from the obstacles drive the robot in a safe path to the goal.

Potential functions can also be viewed as a landscape with mountains (generated by the obstacles) and valleys, with the lowest point of the valley representing the robot goal. The robot follows the path along the negative gradient of the potential function which means moving downhill towards the lowest point in the valley. With this analogy, it is clear that the robot may be trapped in local minima away from the goal, this being a known drawback of the original version of potential field based methods.

Let q represent the position of the robot, considered as a particle moving in a n-dimensional space R^n. For the sake of presentation simplicity consider the problem applied to a point robot moving in a plane, i.e., $n = 2$ and that the robot's pose is defined by the tuple $q = (x, y)$.

The artificial potential field where the robot moves is a scalar function $U(q)$:

$R^2 \longrightarrow R$ generated by the superposition of attractive and repulsive potentials

$$U(q) = U_{att}(q) + U_{rep}(q). \tag{1}$$

The repulsive potential results from the superposition of the individual repulsive potentials generated by the obstacles, and so (1) may be written as

$$U(q) = U_{att}(q) + \sum_i U_{rep_i}(q) \tag{2}$$

where $U_{rep_i}(q)$ represents the repulsive potential generated by obstacle i.

Consider now that $U(q)$ is differentiable. At each q, the gradient of the potential field, denoted by $\nabla U(q)$, is a vector that points in the direction that locally maximally increases $U(q)$. In the potential field based robot navigation methods, the attractive potential is chosen to be zero at the goal and to increase as the robot is far away from the goal and the repulsive potential, associated with each obstacle, is very high (infinity) in the close vicinity of the obstacles and decreases when the distance to the obstacle increases. Along these principles, different attractive potentials may be chosen.

Furthermore, the force that drives the robot is the negative gradient of the artificial potential, i.e.,

$$F(q) = F_{att}(q) + F_{rep}(q) = -\nabla U_{att}(q) - \nabla U_{rep}(q) \tag{3}$$

The force $F(q)$ in (3) is a vector that points in the direction that, at each q, locally maximally decreases U. This force can be considered as the velocity vector that drives the point robot.

The Attractive Potential

The usual choice for the attractive potential is the standard parabolic that grows quadratically with the distance to the goal,

$$U_{att}(q) = \frac{1}{2}\, k_{att}\, d^2_{goal}(q) \tag{4}$$

where $d_{goal}(q) = \| q - q_{goal} \|$ is the Euclidean distance of the robot (considered at q), to the goal, at q_{goal} and k_{att} is a scaling factor. The gradient,

$$\nabla U_{att}(q) = k_{att}(q - q_{goal}) \tag{5}$$

is a vector field proportional to the difference from q to q_{goal} that points away from q_{goal}. The farther away the robot is from the goal, the bigger the magnitude of the

attractive vector field. The attractive force considered in the Potential Filed based approach is the negative gradient of the attractive potential

$$F_{att}(q) = -\nabla U_{att}(q) = -k_{att}\ (q - q_{goal}) \tag{6}$$

Setting the robot velocity vector proportional to the vector field force, the force (6) drives the robot to the goal with a velocity that decreases when the robot approaches the goal. The force (6) represents a linear dependence towards the goal, which means that it grows with no bound as q moves away from the goal which may determine a fast robot velocity whenever far from the q_{goal}. When the robot is far away from the goal, this force imposes that it quickly approaches the goal, i.e., that it moves directly to the goal with a high velocity. On the contrary, the force tends to zero, and so does the robot velocity, when the robot approaches the goal. Therefore the robot approaches the goal slowly which is a useful feature to reduce the overshoot at the goal.

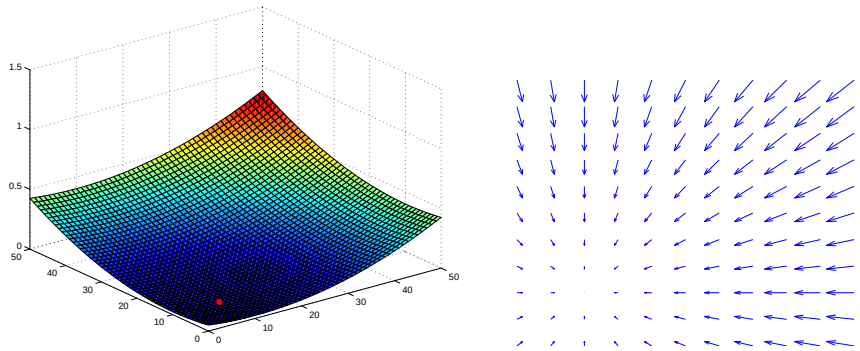

Figure 3: a) Attractive Potential, b) Attractive Force to the goal

Figure 3 represents the attractive potential and the negative gradient force field for a situation where the goal at $(10, 10)$ is represented by a mark.

The Repulsive Potential

The repulsive potential keeps the robot away from the obstacles, both those a priori know or those detected by the robot on-board sensors. This repulsive potential is stronger when the robot is closer to the obstacle and has a decreasing influence when the robot is far away. Given the linear nature of the problem, the repulsive potential results from the sum of the repulsive effect of all the obstacles, i.e.,

$$U_{rep}(q) = \sum_i U_{rep_i}(q) \tag{7}$$

It is reasonable to consider that the influence of an obstacle is limited to the environment space in its vicinity up to a given distance. An obstacle very far from the

robot is not likely to repel the robot. Moreover, the magnitude of repulsive potential should increase when the robot approaches the obstacle. To account for this effect and to the space bounded influence, a possible repulsive potential generated by obstacle i is

$$U_{rep_i}(q) = \begin{cases} \frac{1}{2}k_{obst_i}\left(\frac{1}{d_{obst_i}(q)} - \frac{1}{d_0}\right)^2 & if \quad d_{obst_i}(q) < d_0 \\ 0 & if \quad d_{obst_i}(q) \geq d_0 \end{cases} \tag{8}$$

where $d_{obst_i}(q)$ is the minimal distance from q to the obstacle i, k_{obst_i} is a scaling constant and d_0 is the obstacle influence threshold.

The negative of the gradient of the repulsive potential, $F_{rep_i}(q) = -\nabla U_{rep_i}(q)$, is given by,

$$F_{rep_i}(q) = \begin{cases} k_{obst_i}\left(\frac{1}{d_{obst_i}(q)} - \frac{1}{d_0}\right)\frac{1}{d^2_{obst_i}(q)}\frac{q-q_{obst}}{d_{obst_i}} & if \quad d_{obst_i}(q) < d_0 \\ 0 & if \quad d_{obst_i}(q) \geq d_0 \end{cases} \tag{9}$$

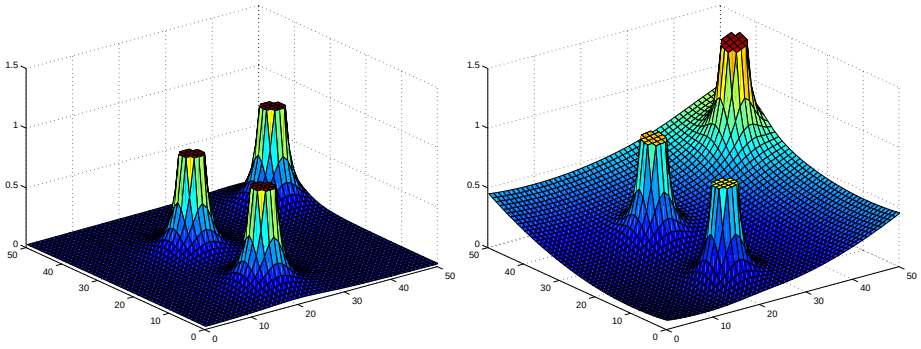

Figure 4: a) Repulsive Potential, b) Attractive+Respulsive Potential

For the environment where the goal lead to the attractive potential represented in Figure 3, the repulsive potential for three obstacles is represented in Figure 4-a), while the sum of the attractive and repulsive potentials is plotted at Figure 4-b). Taking this example, it is clear that the motion of a point robot to the goal, starting in an arbitrary position, can be viewed as the motion of a frictionless ball that is left at the robot starting point. The ball path is along the largest negative slope to the goal.

Advantages and Drawbacks

The potential field approach herein presented is a simple path planning technique that has an intuitive operation principle based on energy type fields. For a static and completely known environment, the potential can be evaluated off-line

providing the velocity profile to be applied to a point robot moving in the energy field from a starting point to a goal. Moreover, the technique can be applied in an on-line version that accommodates an obstacle avoidance component. The repulsive potential may result from known environment obstacles present in an a priori map or obstacles that are detected by the robot on-board sensors during its motion.

In its simplest version the potential field based methods exhibit many shortcomings, in particular the sensitivity to local minima, that usually arise due to the symmetry of the environment and to concave obstacles, and robot oscillatory behavior when traversing narrow spaces.

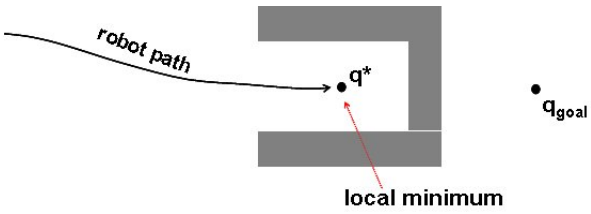

Figure 5: Local minimum of the total potential due to a concave obstacle

Figure 5 presents a situation where the robot is attracted by the goal while approaching a concave obstacle. When inside the concave obstacle, it happens that in a particular position, q^*, the attractive force to the goal is symmetric to the repulsive force due to the obstacle surfaces, this leading to a local minimum of $U(q^*)$, i.e., $\nabla U(q^*) = 0$. Attraction to local minimum of the potential also arises with non-concave obstacles as represented in Figure 6 where the total repulsive force due to the two obstacles is symmetric to the attractive force due to the goal.

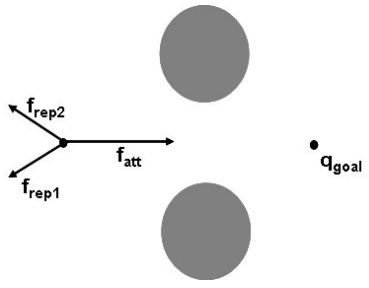

Figure 6: Local minimum of the total potential due to environment symmetry

A large number of improvements and extensions of the potential field have

been published since the early version presented by O. Khatib in [3]. M. Khatib and Chatila in [10] proposed an extended version of the potential field based methods, where the repulsive potential is changed in two different ways. The repulsive force due to an obstacle is not only considered as a function of the distance to the obstacle but also of the orientation of the robot relative to the obstacle. This is a reasonable change since the urgency of avoiding an obstacle parallel to the robot motion is clearly less than the one that arises when the robot moves directly facing the obstacle. The second extension of the repulsive potential does not consider the obstacles that will not closely affect the robot velocity. For example, it is irrelevant to consider the repulsive force generated by an obstacle in the back of the robot, when it is moving forward.

2:3 The Vector Field Histogram

The Vector Field Histogram (VFH) method, introduced by Borenstein and Korem, [4], is a real-time obstacle avoidance method that permits the detection of unknown obstacles and avoids collisions while simultaneously steering the mobile robot towards the target.

The original paper on VFH, [4], presents a good summary of the method as follows: the VFH method uses a two-dimensional Cartesian histogram grid as a world model. This world model is updated continuously with range data sampled by on-board range sensors. The VFH method subsequently employs a two-stage data-reduction process in order to compute the desired control commands for the vehicle. In the first stage, a constant size subset of the 2D histogram grid considered around the robot's momentary location, is reduced to a one-dimensional polar histogram. Each sector in the polar histogram contains a value representing the polar obstacle density in that direction. In the second stage, the algorithm selects the most suitable sector from among all polar histogram sectors with a low polar obstacle density, and the steering of the robot is aligned with that direction.

The three main steps of implementation of the VFH method are summarized:

Step 1 Builds a 2D Cartesian histogram grid of obstacle representation,

Step 2 From the previous 2D histogram grid, considers an active window around the robot, and filters that 2D active grid onto a 1D polar histogram,

Step 3 Calculates the steering angle and the velocity controls from the 1D polar histogram, as a result of an optimization procedure.

Step 1 of VHF

Step 1 of VHF generates a 2D Cartesian coordinate from each range sensor measurement and increments that position in a 2D Cartesian histogram grid map C. The construction of this grid maps does not depend on the specific sensor used for obstacle detection, in particular ultrasound and laser range sensors may be used.

For ultrasound sensors and for each range reading, the cell that lies on the acoustic axis and corresponds to the measured distance d is incremented (see Figure 7), increasing the certainty value (CV) of the occupancy of that cell. This is the Histogrammic in Motion Mapping (HIMM) algorithm presented in [11].

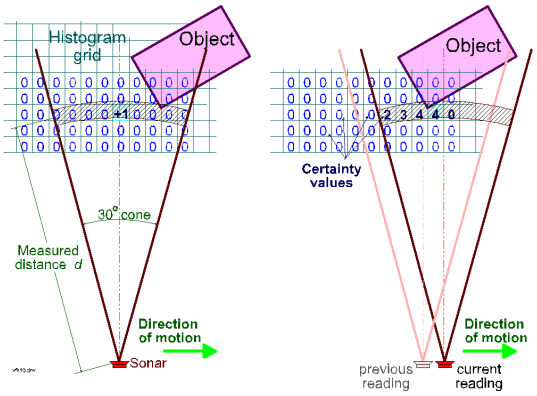

Figure 7: Construction of the 2D Histogram grid map. Reproduced from [4]

Figure 7 illustrates the cells certainty value update along the movement of a robot equipped with ultrasonic sensors. It is clear that, for each range reading, only one cell is updated. The HIMM provides a histogramic pseudo-probability distribution by continuous and rapid sampling the sensors while the robot is moving. This is different from the certainty grid maps proposed by Moravec and Elfes in [12], [13], that project a probability profile onto all the cells affected by a range reading. For an ultrasound sensor these cells are contained in a cone that corresponds to the main lobe of the sensor radiation diagram.

Step 2 of VHF

The next step of VFH, maps the 2D Cartesian histogram grid map C onto a 1D structure. To preserve and isolate the information about the local obstacle information rather than using the entire grid map C, the 2D grid used in this step is restricted to a window of C, called the active window, denoted by C^*, with constant dimensions, centered on the Vehicle Central Point (VCP) and that, consequently, moves with the robot. C^* represents a local map of the environment around the robot.

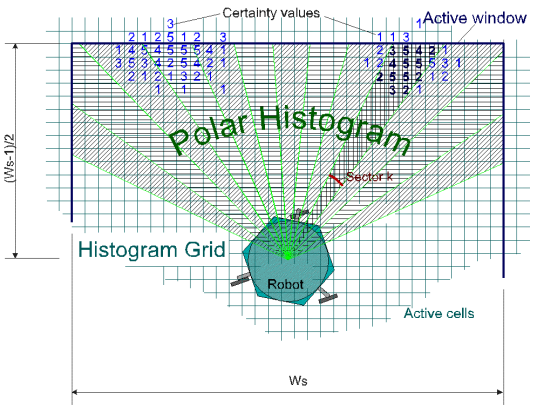

Figure 8: Mapping of active cells onto the polar histogram. Reproduced from [4]

The active grid C^* is mapped onto a 1D structure known as a polar histogram, H, that comprises n angular sections each with width α. Figure 8 illustrates the cell occupancy of C^*, the active window around the robot, and represents the angular sectors considered for the evaluation of the 1D polar histogram.

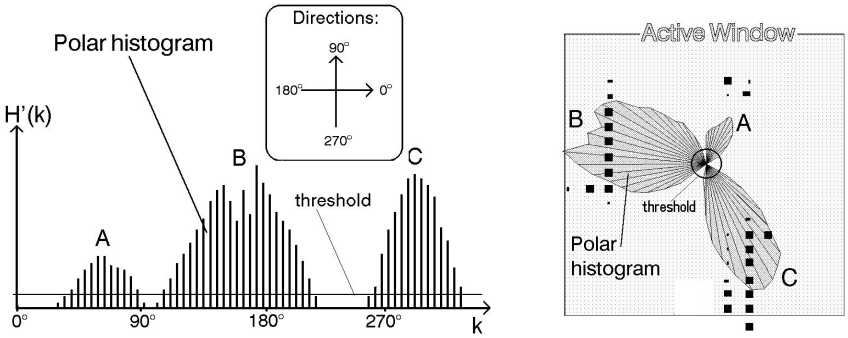

Figure 9: a) 1D polar histogram of obstacle occupancy around the robot. b) Polar histogram shown in polar form overlapped with C^*. Both Reproduced from [4]

The x-axis of the polar histogram represents the angular sector where the obstacles were found and the y-axis represents the probability P that there is really an obstacle in that direction based on the occupancy grid's cell values of C^*. Figure 9-a) represents the 1D polar histogram with obstacle density for a situation where the robot has three obstacles, A, B and C in its close vicinity. In Figure 9-b) the previously obtained 1D histogram is shown in polar form overlapped with the referred obstacles.

Step 3 of VHF

The step 3 of VFH evaluates the required steering direction for the robot that corresponds to a given sector of the 1D histogram and, simultaneously, adapts the robot velocity according to the obstacle polar density.

A typical polar histogram contains ”peaks” or sectors with a high polar density and ”valleys”, i.e., sectors with low polar density. To evaluate the steering direction towards the target goal, all openings, i.e., valleys large enough for the vehicle to pass through, are identified as candidate valleys. Valleys are classified as wide or narrow according to the number of sectors below the threshold. If the number of consecutive sectors below the threshold is greater than S_{max} the valley is wide, while it is classified as narrow if that number is less than S_{max}. The parameter S_{max} is set according to the robot dimensions and kinematic constraints.

From the set of wide valleys, VHF chooses the one that minimizes a cost function that accounts for:

- the alignment of the robot to the target,
- the difference between the robot current direction and the goal direction,
- the difference between the robot previously selected direction and the new robot direction.

If the threshold is set too high, the robot may be too close to an obstacle, and moving too quickly in order to prevent a collision. On the other hand, if set too low, VHF can miss some valid candidate valleys. As stated in [4] the VHF needs a fine-tuned threshold only for the most challenging applications, for example, travel at high speed and in densely cluttered environments. Under less demanding conditions the system performs well even with an imprecisely set threshold. One way to optimize performance is to use an adaptive threshold. Besides the robot steering direction, the VFH also sets the robot speed according to the obstacle polar density, [4].

Advantages and Drawbacks

The Vector Field Histogram overcomes some of the limitations exhibited by the potential field methods. In fact, the influence of bad sensor measurements is minimized because sensorial data is averaged out onto an histogram grid that is further processed. Moreover, instability in travelling down a corridor, present when using the potential field method, is eliminated because the polar histogram varies only slightly between sonar readings. In the VFH there is no repulsive nor attractive forces and thus the robot cannot be trapped in a local minima, because VFH only tries to drive the robot through the best possible valley, regardless if it leads away from the target.

Enhanced versions of the VHF method are presented in [14] and [15].

References

[1] V. Lumelsky and T. Skewis, "Incorporating range sensing in the robot navigation function," *IEEE Transactions on Systems Man and Cybernetics*, vol. 20, pp. 1058 – 1068, 1990.

[2] V. Lumelsky and Stepanov, "Path-planning srategies for a point mobile automaton amidst unknown obstacles of arbitrary shape," *in Autonomous Robots Vehicles, I.J. Cox, G.T. Wilfong (Eds), New York, Springer*, pp. 1058 – 1068, 1990.

[3] O. Khatib, "Real-time obstacle avoidance for manipulators and mobile robots," *International Journal of Robotics Research*, vol. 5, no. 1, pp. 90–98, 1995.

[4] J. Borenstein and Y. Koren, "The vector field histogram - fast obstacle avoidance for mobile robots," *IEEE Transaction on Robotics and Automation*, vol. 7, no. 3, pp. 278 – 288, 1991.

[5] S. Quinlan and O. Khatib, "Elastic bands: Connecting path planning and control," *in Proceedings of the IEEE Conference on Robotics and Automation*, pp. 802 – 807, 1993.

[6] E. Bicho and G. Schoner, "The dynamic approach to autonomous robotics demonstrated on a low-level vehicle platform," *Robotics and Autonomous Systems*, vol. 21, pp. 23 – 35, 1997.

[7] E. Bicho, *Dynamic Approach to Behavior-Based Robotics: design, specification, analysis, simulation and implementation*. Shaker Verlag, 2000.

[8] H. Choset and all, *Principles of Robot Motion: theory, algorihms and implementations*. Englewood Cliffs and New Jersey: MIT Press, 2005.

[9] I. Kamon, E. Rimon, and E. Rivlin, "A range-sensor based navigation algorithm," *International Journal of Robotics Research*, vol. 17, no. 9, pp. 934 – 953, 1991.

[10] M. Khatib and R. Chatila, "An extended potential field approach for mobile robot sensor-based motions," *in Proc. of the Intelligent Autonomous Systems, IAS-4, IOS Press*, pp. 490–496, 1995.

[11] J. Borenstein and Y. Koren, "Histogramic in-motion mapping for mobile robot obstacle avoidance," *IEEE Transaction on Robotics and Automation*, vol. 7, no. 4, pp. 535 – 539, 1991.

[12] H. Moravec and A. Elfes, "High resolution maps from wide angle sonar," *in Proceedings of the IEEE International Conference on Robotics and Automation*, pp. 116 – 121, 1985.

[13] A. Elfes, "Sonar-based real-world mapping and navigation," *IEEE Journal of Robotics and Automation*, vol. RA-3, no. 3, pp. 249 – 265, 1987.

[14] I. Ulrich and J. Borenstein, "Vhf+: Reliable obstacle avoidance for fast mobile robots," *Proc. of the IEEE Int. Conf. on Robotics and Automation*, pp. 1572 – 1577, 1998.

[15] ——, "Vhf+: Local obstacle avoidance with look-ahead verification," *Proc. of the IEEE Int. Conf. on Robotics and Automation*, pp. 2505 – 2511, 2000.